Interaction between randomly charged rods and plates: Energy landscapes, stick slip, and recognition at a distance

Sergei Panyukov* and Yitzhak Rabin
Department of Physics, Bar-Ilan University, Ramat-Gan 52900, Israel
(Received 12 May 1997)

We study the interaction between randomly, irreversibly charged objects. We consider arbitrary relative displacements of two parallel rigid rods and of two parallel rigid plates, and calculate the statistical properties of the resulting energy landscape, such as the distribution of the energies of potential minima and maxima, the depth, the radia of curvature, and the width and density of typical energy wells, as functions of the separation between the objects and of the Debye screening length. We show that this complicated energy landscape may lead to stick-slip phenomena during relative displacement of the plates. We study the case of perfectly correlated charge distributions on the two objects, and show that the presence of long range forces may lead to prealignment of the objects, even before contact. The relevance of our results to interacting biological systems and to pattern recognition is discussed. [S1063-651X(97)11812-8]

PACS number(s): 61.43.−j, 68.35.−p

I. INTRODUCTION

The statistical physics of interacting many-body systems deals with a thermodynamically large number of elementary units (atoms, spins, etc.), each of which is described by a small number of parameters. This leads to a class of models in which complex physical behavior arises due to cooperative behavior of a large number of such ''simple'' units.

In this work we consider a different class of interacting systems, namely, that in which the number of parameters necessary to specify a single unit is very large. Due to the inherent complexity of the individual units, even a small number of such interacting objects can exhibit very complex behavior. A generic system of this type consists of interacting objects on which a random distribution of charges is irreversibly placed. From the viewpoint of information theory, such objects are of ''maximal complexity'' in the sense that complete specification of the charge distributions requires precise information about the location of each of the charges, the number of which can be arbitrary large, depending on the size of the objects. In such systems, complex behavior can already be observed at the level of two interacting systems, the case considered in the present work.

Aside from its maximal complexity, the motivation for the choice of a random distribution of the frozen charges is twofold. First, it is known that many biological systems, such as proteins, can be described as nearly random assemblies of their constituents [1] (amino acids), each of which interacts in a different way with its environment. The resulting potential energy surface that exists in the vicinity of a folded protein is extremely complicated. Since a random combination of positive and negative charges interacting through screened Coulomb forces can give rise to potential surfaces of nearly arbitrary complexity, the theory presented in this work can be considered as the simplest minimal model of interaction between such ''proteins.'' Second, the frozen randomness assumption allows us to use some of the powerful mathematical machinery that was developed for the study of systems with quenched disorder [2,3].

A well known problem in polymer physics which appears to be close to the present one is that of random block copolymers [4]. One difference between the random copolymer models and the model studied in the present work stems from the fact that long range interactions considered here are usually not taken into account in the former class of models. More importantly, while we consider rigid objects (rods and plates), standard copolymer (and polyampholyte [5]) models are based on the assumption that the ''charges'' are placed on flexible chains and, therefore, while the linear structure of the polymers in these models is ''quenched,'' their three-dimensional structure is ''annealed'' (at least in the high temperature phase). In this sense random block copolymer theories can be thought of as generic models for the folding of proteins, while our theory of interacting rigid objects attempts to capture some of the features of the way folded proteins interact with their environment.

In Sec. II we introduce the model of randomly and irreversibly charged objects interacting through arbitrary long range potentials. The distribution function (number density) of the energy minima generated by the relative displacement of the two objects is defined and replaced by its average over the quenched ensemble (this replacement is justified in the Appendix). In the following sections we consider two geometries: interacting parallel rods and interacting parallel plates. Although other geometries are also analytically tractable and will be considered in the future, the introduction of nonparallel orientations, and of other geometrical shapes, increases the number of free parameters and obscures the basic physics of the problem.

In Sec. III we calculate the distribution function of energy minima for the case of two parallel randomly charged rods. We proceed to examine the statistical properties of the interaction energy landscape as a function of the distance between the rods, and calculate the depths, the radii of the curvature, and the widths of the energy minima and maxima,

*Permanent address: Theoretical Department, Lebedev Physics Institute, Russian Academy of Sciences, Moscow 117924, Russia.

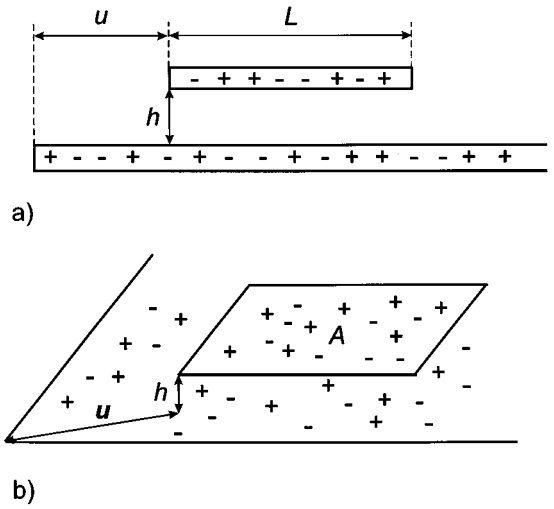

FIG. 1. Schematic drawing of (a) two randomly charged parallel rods, one of length L and the other infinite, separated by a vertical distance h and displaced by a distance u. (b) A similar drawing of two plates, one of area A and the other infinite.

and the average distance between them. Explicit results for the above quantities are obtained for randomly frozen charge distributions interacting via screened Coulomb forces. We study the variation of the position of a given minimum as a function of the separation between the rods.

In Sec. IV we carry out a similar program for interacting randomly charged plates. We then apply our general results to the study of the stick-slip problem, and estimate the critical force which has to be applied in order to produce relative displacement of the two plates. In Sec. V we study the energy landscape of perfectly correlated charge distributions (mirror images) on the two plates, and discuss the possibility of prealignment as they approach each other. The effect of partial correlation of the two charge distributions is also considered. In Sec. VI we discuss the main results of this work, and speculate on their relevance to interacting biological systems, random magnetic films, pattern recognition, etc.

II. MODEL

Consider two objects (two rigid rods or plates) on which positive and negative charges with local charge densities $\rho_{i+}(\mathbf{x})$ and $\rho_{i-}(\mathbf{x})$ (the index i takes the values 1 and 2, corresponding to the two objects) are randomly and irreversibly placed. The frozen (quenched) distribution of total charge is given by $\rho_i(\mathbf{x})=\rho_{i+}(\mathbf{x})-\rho_{i-}(\mathbf{x})$ $(i=1,2)$. The charges on the two objects interact via a potential V (for example, a screened Coulomb potential). We assume that the two objects are parallel and separated by a distance h from each other and are allowed to undergo parallel displacement by a vector $\mathbf{u}$, with respect to some arbitrary origin of coordinates (Fig. 1). The interaction energy (which does not include the constant self-energy of the rods or plates) is given by

$$E(\mathbf{u})=\int\int d\mathbf{x}_1 d\mathbf{x}_2 \rho_1(\mathbf{x}_1)\rho_2(\mathbf{x}_2)V(\mathbf{x}_1-x_2-\mathbf{u}), \quad (1)$$

where the integration is taken over all the points in the two objects. We assume that the potential $V(\mathbf{x}_1-\mathbf{x}_2-\mathbf{u})$ depends only on the distance $r=[(\mathbf{x}_1-\mathbf{x}_2-\mathbf{u})^2+h^2]^{1/2}$ between the points $\mathbf{x}_1$ and $\mathbf{x}_2+\mathbf{u}$ on the two objects, and decays sufficiently rapidly with r.

The assumption that the charges are randomly distributed on the rods (plates), with average charge density $\overline{\rho}=\overline{\rho_+}-\overline{\rho_-}$, leads to a Gaussian distribution of the quenched variations of density $\delta\rho_i(\mathbf{x})=\rho_i(\mathbf{x})-\overline{\rho}$, with the second moment

$$\overline{\delta\rho_i(\mathbf{x})\,\delta\rho_j(\mathbf{x}')}=g\,\delta_{ij}\delta(\mathbf{x}-\mathbf{x}'), \quad (2)$$

where $g\equiv\overline{\rho_+}+\overline{\rho_-}$ is the number density of charges, and the bar denotes averaging over the ensemble of all possible realizations of quenched disorder on the rods, with the probability distribution

$$W[\delta\rho]=\mathcal{N}^{-1}e^{-S[\delta\rho]}, \quad (3)$$

where

$$S[\delta\rho]\equiv\int d\mathbf{x}\,\frac{\delta\rho^2(\mathbf{x})}{2g}, \quad (4)$$

and

$$\mathcal{N}\equiv\int D[\delta\rho]e^{-S[\delta\rho]} \quad (5)$$

is the normalization factor ($\int D[\delta\rho]$ denotes functional integration over the density variations).

In order to avoid complications associated with the change of overlap between the two rods of lengths L and L' (or two plates of areas A and A') upon parallel displacement, we assume that $L\ll L'$, and consider only relative displacements for which the two rods overlap (a similar assumption, $A\ll A'$, is made for the case of two plates). The energy $E(\mathbf{u})$ associated with a particular relative shift of the two objects differs, in general, from the average interaction energy $\overline{E}$,

$$\overline{E}=\overline{\rho}^2M\int d\mathbf{x}\,V(\mathbf{x}), \quad (6)$$

by an amount $\delta E(\mathbf{u})=E(\mathbf{u})-\overline{E}$. Here M corresponds to the length L or to the area A, in the one (rods) and the two-dimensional (plates) case, respectively, and the remaining integration is over the coordinates of the larger object (L' and A' in the rod and the plate case, respectively). In Fig. 2 we plot a typical energy landscape $\delta E(u)$ which results from the relative shift u of two rods (this plot was generated by a computer simulation of the randomly frozen charge distributions on the rods, with periodic boundary conditions).

The number of energy minima (''potential wells'') $N_{\min}(E)\Delta E$ with energy in the interval $(E,E+\Delta E)$ can be obtained from the expression

$$N_{\min}(E)=\sum_{\text{extr}}\delta[E-\delta E(\mathbf{u})]\theta[\Lambda_-(\mathbf{u})], \quad (7)$$

where the sum goes over the positions $\mathbf{u}$ of all the energy extrema, each of which is defined by the relation

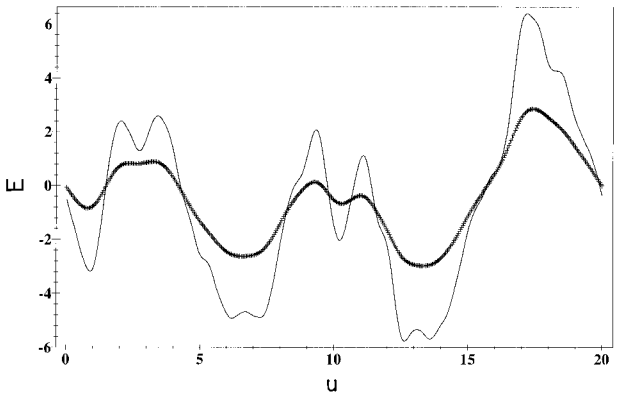

FIG. 2. Plot of the energy landscape $\delta E(u)$ (in units of $gL^{1/2}$) as a function of the relative displacement u (in arbitrary units of length), for a randomly chosen realization of disordered charge distributions on the rods. The solid line corresponds to $h=1$, and the crosses correspond to $h=0.5$.

$\partial \delta E(\mathbf{u})/\partial \mathbf{u}=0$. The θ function in this expression ensures that only energy minima are counted among all extrema. For two parallel rods, u is a scalar and $\Lambda_-(u)=\partial^2 \delta E(u)/\partial u^2$ is the inverse squared radius of curvature of the energy minimum, which is a measure of the ''stiffness'' of the effective ''spring constant'' associated with the potential well. In the case of two parallel plates $\mathbf{u}$ is a two-dimensional vector, and $\Lambda_-(\mathbf{u})$ is defined as the minimal eigenvalue of the matrix of second variations of the energy (1), with components

$$E_{\alpha\beta}(\mathbf{u}) \equiv \frac{\partial^2[\delta E(\mathbf{u})]}{\partial u_\alpha \partial u_\beta}. \tag{8}$$

This minimal eigenvalue is given by

$$\Lambda_- = E_+ - \sqrt{E_-^2 + E_{xy}^2}, \quad E_\pm \equiv \frac{E_{xx} \pm E_{yy}}{2}. \tag{9}$$

Note that if we change the sign of the potential V, the minima and maxima of the energy are interchanged. This means that the distribution of the energy maxima is determined by the same function, Eq. (7), with the substitution $N_{\max}(E)=N_{\min}(-E)$. In the two-dimensional case the extrema of the energy include saddle points, and, in order to carry out a complete classification of the extrema, we have to introduce the maximum eigenvalue of the matrix (8),

$$\Lambda_+ = E_+ + \sqrt{E_-^2 + E_{xy}^2} \geqslant \Lambda_- . \tag{10}$$

We can identify Λ_- and Λ_+ with *inverse squared radii of curvature* of the potential wells along the principal axes of curvature. The case $\Lambda_->0$ corresponds to energy minima, $\Lambda_+<0$ to maxima, and $\Lambda_-<0$, $\Lambda_+>0$ to saddle points.

Since the sum in Eq. (7) goes over regions with different quenched disorder, for large enough rods and plates we can make the replacement $N_{\min}(E) \to \overline{N_{\min}(E)}$, where the bar denotes averaging over the ensemble of different realizations of the quenched charge distributions on the objects (the justification for this replacement is given in the Appendix):

$$\overline{N_{\min}(E)} = \overline{\sum_{\text{extr}} \delta[E-\delta E(\mathbf{u})]\,\theta[\Lambda_-(\mathbf{u})]}. \tag{11}$$

The expression on the right hand side of this equation is averaged over the distribution of the charge density $\delta\rho_2$ on one of the objects with the probability $W[\delta\rho_2]$, Eq. (3). We would like to stress that the number of energy minima is determined only by the statistical properties of the frozen charge distributions, and does not depend on temperature (temperature effects and the kinetics of interacting objects are not considered in this work). We now proceed to discuss the energy landscape of two parallel rods.

III. PARALLEL RODS

A. Distribution of energy minima

The sum over the positions u of energy extrema in Eq. (11) can be transformed into an integral over the continuous variable u,

$$\sum_{\text{ext}} \cdots = \int du \sum_{\text{ext}} \delta(u-u_{\text{ext}}) \cdots$$

$$= \int du\ \delta\{\partial[\delta E(u)]/\partial u\} \left|\partial^2[\delta E(u)]/\partial u^2\right| \ldots, \tag{12}$$

where u_{ext} are the solutions of the equation $\partial[\delta E(u)]/\partial u = 0$ (in general, many such solutions exist). In order to deal with the θ function in Eq. (11) we represent it in the form

$$\theta(\Lambda_-[\mathbf{u}]) = \int_0^\infty d\Lambda\ \delta\left\{\Lambda - \frac{\partial^2[\delta E(u)]}{\partial u^2}\right\}. \tag{13}$$

Substituting Eqs. (13) and (12) into Eq. (11), and changing the order of averaging over $\delta\rho_2$ and integration over u (which gives the length L' of the ''infinite'' rod), we obtain the following representation for the energy distribution function:

$$\overline{N_{\min}(E)} = L' \int_0^\infty d\Lambda\ \Lambda\ \frac{1}{\mathcal{N}} \int D[\delta\rho_2] e^{-S[\delta\rho_2]}$$

$$\times \delta\{\partial[\delta E(u)]/\partial u\}\,\delta[E-\delta E(u)]\,\delta\{\Lambda$$

$$- \partial^2[\delta E(u)]/\partial u^2\}. \tag{14}$$

The standard way of handling such integrals is to use the exponential representation of the δ functions

$$\delta[E-\delta E(u)] = \int \frac{dk_1}{2\pi} \exp\{ik_1[E-\delta E(u)]\},$$

$$\delta\left\{\frac{\partial[\delta E(u)]}{\partial u}\right\} = \int \frac{dk_2}{2\pi} \exp\left\{-ik_2 \frac{\partial[\delta E(u)]}{\partial u}\right\}, \tag{15}$$

$$\delta\left\{\Lambda - \frac{\partial^2[\delta E(u)]}{\partial u^2}\right\} = \int \frac{dk_3}{2\pi} \exp\left\{ik_3\left[\Lambda - \frac{\partial^2[\delta E(u)]}{\partial u^2}\right]\right\}.$$

Substituting these expressions into Eq. (14), we can perform the Gaussian integration over the density distribution $\delta\rho_2(x)$ by shifting the variable of integration $\delta\rho_2(x) \to \delta\rho_2(x) + \delta\rho_2^*(x)$, where $\delta\rho_2^*$ is defined by

$$\delta\rho_2^*(x)\equiv -ig\int dx' K(x-x'-u)\,\delta\rho_1(x') \tag{16}$$

and

$$K(x)=k_1V(x)+k_2\partial V(x)/\partial x+k_3\partial^2V(x)/\partial x^2. \tag{17}$$

Substituting Eq. (16) into the definition of $S[\delta\rho_2]$, we observe that the product $\delta\rho_1(x)\,\delta\rho_1(x')$ in the integral over the coordinates x and x' can be replaced by its average over the length of the rod. In the ''thermodynamic'' limit (the length of the shorter rod L is much larger than the average spacing between the charges on the rod, $1/g$) we can replace the latter average by the quenched average (2),

$$\delta\rho_1(x)\,\delta\rho_1(x')\rightarrow\overline{\delta\rho_1(x)\,\delta\rho_1(x')}=g\,\delta(x-x'), \tag{18}$$

and arrive at the expression

$$\overline{N_{\min}(E)}=L'\int_0^\infty d\Lambda\ \Lambda\prod_{j=1}^{3}\int\frac{dk_j}{2\pi}\times\exp\left[ik_1E+ik_3\Lambda-\frac{g^2L}{2}\sum_{jl}D_{jl}k_jk_l\right], \tag{19}$$

where the matrix $\mathbf{D}$ has the form

$$\mathbf{D}=\begin{pmatrix} m_0(h) & 0 & -m_1(h)\\ 0 & m_1(h) & 0\\ -m_1(h) & 0 & m_2(h)\end{pmatrix}. \tag{20}$$

The quantities $m_n(h)$ $(n=0,1,2,...)$ are the second moments of the nth derivatives of the potential,

$$m_0(h)\equiv 2\int_0^\infty dr\ V^2(r),\quad m_1(h)\equiv 2\int_0^\infty dr\left[\frac{\partial V(r)}{\partial r}\right]^2,\quad m_2(h)\equiv 2\int_0^\infty dr\left[\frac{\partial^2V(r)}{\partial r^2}\right]^2. \tag{21}$$

Performing the Gaussian integration over variables k_j in Eq. (19), we obtain

$$\overline{N_{\min}(E)}=L'\overline{c}\int_0^\infty d\Lambda\ \mathcal{P}(\Lambda)P(E|\Lambda). \tag{22}$$

Here $\overline{c}$ is the average concentration of potential wells (number of potential minima per unit length of the rod of length L') for parallel rods separated by a distance h

$$\overline{c}=\frac{1}{2\pi}\left(\frac{m_2(h)}{m_1(h)}\right)^{1/2}, \tag{23}$$

Note that the average distance between potential wells is given by $1/\overline{c}$. For unscreened Coulomb interaction between the rods, one can show that $m_1\sim 1/h^3$ and $m_2\sim 1/h^5$, and thus $\overline{c}\sim 1/h$ (i.e., the distance between the energy minima is of order h). We conclude that the density of energy minima increases with decreasing separation between the rods, and approaches the number density of charges g at a distance $h\simeq 1/g$ which corresponds to the limit of validity of our model (at such separations the charge distribution can no longer be considered as continuous). At this point the number of potential energy minima $L'\overline{c}$ approaches the total number of charges on the infinite rod, $L'g$.

In the case of screened Coulomb interaction between the charges, the potential V given by

$$V(r)=\frac{e^{-\kappa\sqrt{r^2+h^2}}}{\sqrt{r^2+h^2}}, \tag{24}$$

where κ^{-1} is the Debye screening length (we set the constant coefficient in front of this expression to unity). The qualitative picture discussed in the preceding paragraph remains valid in the range $g^{-1}<h<\kappa^{-1}$. A straightforward calculation shows that in the limit of strong screening $(\kappa h\gg 1)$, $m_1\sim\kappa^{1/2}h^{-5/2}\exp(-2\kappa h)$ and $m_2\sim\kappa^{3/2}h^{-7/2}\exp(-2\kappa h)$, and therefore $\overline{c}\sim(\kappa/h)^{1/2}$. The conclusion that the concentration of energy minima at distances exceeding the screening length is larger in the screened than in the unscreened Coulomb case, is quite unexpected. However, as will be shown in the following, the energy of these potential wells is exponentially reduced by screening effects.

The function $\mathcal{P}(\Lambda)$ which appears in Eq. (22), is the probability of finding an energy minimum with a given stiffness (inverse squared radius of curvature) Λ

$$\mathcal{P}(\Lambda)=\frac{\Lambda}{g^2Lm_2(h)}\exp\left[-\frac{\Lambda^2}{2g^2Lm_2(h)}\right]. \tag{25}$$

This function has a maximum at $\Lambda_{\max}=g[Lm_2(h)]^{1/2}$ and decays to zero for both large and small radii of curvature. The function $P(E|\Lambda)$ which also appears in Eq. (22) is the conditional probability to find a minimum with energy E, given that its stiffness is Λ,

$$P(E|\Lambda)=\frac{1}{(2\pi\sigma_E^2)^{1/2}}\exp\left[-\frac{[E-\overline{\delta E}_{\min}(\Lambda)]^2}{2\sigma_E^2}\right]. \tag{26}$$

Here, the average energy of a well with a given stiffness Λ is

$$\overline{\delta E}_{\min}(\Lambda)=-\frac{m_1(h)}{m_2(h)}\Lambda<0, \tag{27}$$

and we conclude that the depth of an energy well increases on the average with its stiffness. Although $\overline{\delta E}_{\min}(\Lambda)$ is negative definite as expected, there is a nonvanishing probability to find a potential well with energy higher than the average energy, i.e., $\delta E>0$. This probability decreases rapidly with the stiffness Λ. The squared deviation of the energy from the average value

$$\sigma_E^2=g^2L[m_0(h)-m_1^2(h)/m_2(h)] \tag{28}$$

does not depend on the well stiffness Λ. For the unscreened Coulomb case, $\sigma_E\simeq g\sqrt{L/h}$, and the spread of the energies of the minima increases as $h^{-1/2}$ when the rods approach each other. In the presence of screening this result is unchanged for distances smaller than the screening length. At larger distances, σ_E decreases exponentially, as $\exp(-\kappa h)$.

Averaging Eq. (27) over Λ with the distribution function (25), we obtain the average well depth

$$\overline{\delta E}_{\min} = -\frac{g m_1(h)}{4}\left(\frac{\pi L}{m_2(h)}\right)^{1/2}. \tag{29}$$

Repeating the same steps for the energy maxima we obtain the average height of energy maxima $\overline{\delta E}_{\max} = -\overline{\delta E}_{\min}$.

Note that $\overline{\delta E}_{\min} \propto \sqrt{L}$, and since for sufficiently large systems the energy of attraction can easily exceed the thermal energy $k_B T$, the frozen randomness of the charge distribution on microscopic scales may result in ''pinning,'' i.e., the system will be trapped in one of the typical energy minima. Such effects can be observed by keeping the rods at a fixed distance and monitoring their stick-slip response to externally applied tangential forces. In order to understand the nature of this response, we need to obtain additional information about the energy landscape generated by a relative translation of the parallel rods. This will be done in the following.

Evaluating the integrals in Eq. (22) in the case of an unscreened Coulomb potential, we find that the function $\overline{N_{\min}(E)}$ can be written in a universal form:

$$\overline{N_{\min}(E)} = \frac{L'}{g\sqrt{hL}}\, p_{\min}\left[\frac{E}{g}\left(\frac{h}{L}\right)^{1/2}\right],$$

where

$$p_{\min}(y) \equiv \frac{\sqrt{2}}{16\pi^2}\exp\left(-\frac{y^2}{2\pi}\right) \times\left[5\exp\left(-\frac{y^2}{25\pi}\right) + y\ \mathrm{erf}\left(\frac{y}{5\sqrt{\pi}}\right) - y\right], \tag{30}$$

where erf is the error function. Expressions of these types are familiar from theories of stochastic processes (e.g., Gaussian random currents). For example, there is an analogy between the current intensity as a function of time and the random interaction energy as a function of relative displacement of the rods. The expression for the probability density function of maxima of the intensity of random noise currents [6] resembles Eq. (30).

In Fig. 3 we plot the number of energy wells per unit energy and unit length, $\overline{N_{\min}}/L'$, as a function of δE, for several values of L/h (for the unscreened Coulomb case). Although the distribution is always peaked at a negative value of δE [see Eq. (29)], there is a finite probability of observing a potential well with a positive value of δE. This reflects the possibility of having local energy minima located inside broad energy maxima (see Fig. 2). Note that the distribution broadens and shifts to more negative values with a closer approach between the rods.

B. Width of the energy minima

The width of a potential well cannot be directly estimated from a knowledge of local characteristics of its minimum, and one has to consider the shape of the energy profile between two neighboring energy extrema. We define the width of the well w as the distance between the position of the minimum and the position of the neighboring maximum. To estimate this value we introduce the number $c(\Lambda|w)$ of wells per unit length with a given stiffness $\Lambda > 0$ and separated by the distance w from a maximum with an arbitrary stiffness $\Lambda' < 0$. Repeating the steps which led to the derivation of Eq. (14), we find the following expression for this conditional probability:

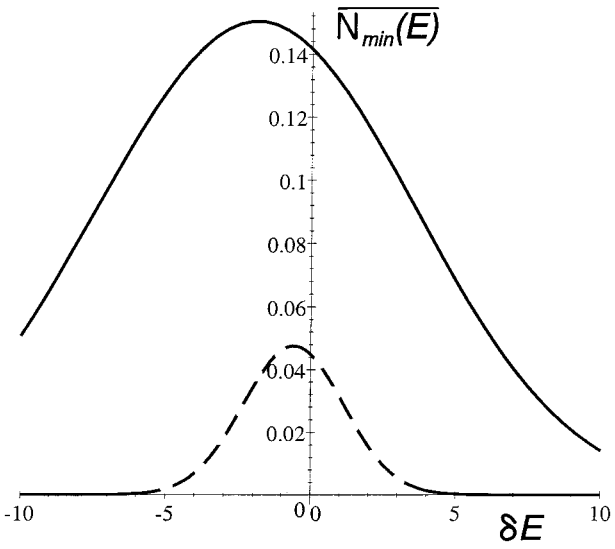

FIG. 3. Plot of the number of minima per unit energy per unit length, $\overline{N_{\min}(E)}/L'$, as a function of the energy δE, for different vertical separations between the rods. The broken line corresponds to $h = L$, and the solid line to $h = 0.1L$ (the density of charges g is unity).

$$\begin{aligned} c(\Lambda|w) &= \int_{-\infty}^{0} d\Lambda' \Lambda|\Lambda'| \frac{1}{\mathcal{N}} \int D[\delta\rho_2] e^{-S[\delta\rho_2]} \\ &\times \delta\{\partial[\delta E(u)]/\partial u\}\,\delta\{\Lambda - \partial^2[\delta E(u)]/\partial u^2\} \\ &\times \delta\{\partial[\delta E(u+w)]/\partial u\}\,\delta\{\Lambda' - \partial^2[\delta E(u+w)]/\partial u^2\}. \end{aligned} \tag{31}$$

The functional integral over $\delta\rho_2(x)$ can be calculated as before, with the result

$$\begin{aligned} c(\Lambda|w) = g^{-4} L^{-2} &[1-\eta_1^2(w)]^{-1/2}[1-\eta_2^2(w)]^{-1/2} \\ &\times \frac{1}{(2\pi)^2 m_1 m_2}\int_{-\infty}^{0} d\Lambda' \Lambda|\Lambda'| \\ &\times \exp\left\{-\frac{\Lambda^2 + (\Lambda')^2 - 2\eta_2(w)\Lambda\Lambda'}{2g^2 L m_2[1-\eta_2^2(w)]}\right\}, \end{aligned} \tag{32}$$

where we defined

$$\begin{aligned} \eta_1(w) &\equiv \frac{1}{m_1}\int_{-\infty}^{\infty} dr\, \frac{\partial V(r)}{\partial r}\,\frac{\partial V(r+w)}{\partial r}, \\ \eta_2(w) &\equiv \frac{1}{m_2}\int_{-\infty}^{\infty} dr\, \frac{\partial^2 V(r)}{\partial r^2}\,\frac{\partial^2 V(r+w)}{\partial r^2}. \end{aligned} \tag{33}$$

Performing the integration over the stiffness of the maxima, Λ', in Eq. (32), and recalling the expressions for the concentration of minima $\overline{c}$, Eq. (23), and for the distribution function of the stiffness of energy minima Λ, Eq. (25), we obtain

$$c(\Lambda|w)=\overline{c}^{2}\mathcal{P}(\Lambda)q(\Lambda|w),$$

where

$$q(\Lambda|w)=\left(\frac{1-\eta_2^2(w)}{1-\eta_1^2(w)}\right)^{1/2}\exp\left[-\frac{\Lambda^2}{g^2Lm_2[\eta_2^{-2}(w)-1]}\right]. \tag{34}$$

In order to obtain some intuition about the dependence of this function on w, we consider two limiting cases. In the limit $w\to\infty$ we obtain $q(\Lambda|w\to\infty)=1$. The presence of the prefactor $\overline{c}^2$ in the above expression for $c(\Lambda|w)$ [the first line in Eq. (34)] expresses the fact that the correlation between minima and maxima disappears in this limit and the joint probability of observing a minimum and a maximum is given by the product of the concentration $\overline{c}\mathcal{P}(\Lambda)\Delta\Lambda$ of energy minima with given Λ and of the concentration of maxima $\overline{c}$ [which is the same as the concentration of minima, Eq. (23)]. In the limit of small w we can expand the integrals in Eq. (33) in powers of w, and obtain

$$q(\Lambda|w)\simeq\frac{\sqrt{m_1m_3}}{m_2}\exp\left(-\frac{\Lambda^2}{w^2g^2Lm_3}\right),\quad w\ll\left(\frac{m_2}{m_3}\right)^{1/2}, \tag{35}$$

where

$$m_3\equiv 2\int_0^\infty dr\left[\frac{\partial^3V(r)}{\partial r^3}\right]^2. \tag{36}$$

Inspection of Eq. (35) shows that the probability of observing an energy minimum and an energy maximum separated by a distance w tends rapidly to zero when $w\to 0$. This confirms the intuitive expectation that a maximum and a minimum cannot coincide. For fixed w this probability decreases rapidly with the stiffness of the minimum, Λ. The reason for this is that stiffer potential wells are characteristically deeper than shallow ones and, as expected, the concentration of shallow minima is much larger than that of deep (and stiff) ones.

The average width $w(\Lambda)$ of a well with curvature Λ can be estimated from the condition that the probability $q(\Lambda|w_\Lambda)$ to find the maximum at a distance w from this well is about one-half (at distances much smaller than this width the probability goes to zero, and at much larger distances it goes to unity). For wells with curvature smaller than the typical one [which corresponds to the maximum of the distribution $\mathcal{P}(\Lambda)$, Eq. (25)], $\Lambda_{\max}=g(Lm_2)^{1/2}$, we can use the asymptotic expression (35) and obtain

$$w(\Lambda)\simeq\frac{\Lambda}{g\sqrt{Lm_3}}. \tag{37}$$

In the opposite limit, $\Lambda\gg\Lambda_{\max}$, the average width of the minima is determined from the equation $\eta_2[w(\Lambda)]=\Lambda_{\max}/\Lambda$. In the unscreened Coulomb case $w(\Lambda)\sim h^{3/2}\Lambda^{1/5}$, i.e., the width of the minimum is a weakly increasing function of its stiffness.

The average width of an energy well is defined as

$$w(\Lambda_{\max})\simeq\left[\frac{m_2(h)}{m_3(h)}\right]^{1/2}. \tag{38}$$

As expected, this average width is of the same order as the average distance between the typical minima, $\overline{c}^{-1}$ [see Eq. (23)], i.e., the *characteristic minima form a densely packed random lattice*. At distances smaller than the screening length the average spacing of this lattice is of the order of the spacing between the rods h and at larger distances it is $(h/\kappa)^{1/2}$. Since both the curvature and the width of shallow energy wells are small, and since the probability to observe uncharacteristically deep wells is exponentially small, the resulting energy landscape does not have a fractal character (i.e., it is smooth).

As a byproduct of the above calculation we can obtain more detailed information about the distribution of extrema in our problem. The integrand in Eq. (31) gives the probability to find two extrema with given inverse radii of curvature Λ and Λ', separated distance w from each other. Integrating this function over positive Λ and Λ', we find the correlation function of concentration of energy wells

$$\overline{c(r)c(r+w)}=\frac{2\overline{c}_1^2[1-\eta_2^2(w)]^{3/2}}{[1+\eta_2^2(w)][1-\eta_1^2(w)]^{1/2}}, \tag{39}$$

which behaves as w^2 on small distances w. The correlation between minima is lost on distances of order of the average spacing between the characteristic energy wells.

C. Dependence of the well parameters on *h*

We now consider what happens with a given energy minimum when we change the distance h between plates by a small value δh. There are two types of changes: the minimum is displaced by the vector $\delta u=(\partial u/\partial h)\delta h$, and its depth and curvature change. Differentiating the equation for the extrema, $\partial[\delta E(u)]/\partial u=0$, with respect to h, and taking into account both the implicit and the explicit dependence of the energy on h, we find

$$\frac{\partial u}{\partial h}=-\frac{\partial^2[\delta E(u)]/\partial u\,\partial h}{\partial^2[\delta E(u)]/\partial u^2}=-\frac{\Theta}{\Lambda}\quad\text{where}\quad\Theta\equiv\frac{\partial^2[\delta E(u)]}{\partial u\,\partial h}. \tag{40}$$

The derivative $\partial u/\partial h$ varies from one well to another, and according to Eq. (40), its distribution for energy minima with a given stiffness Λ is determined by the distribution of the random variable Θ. The distribution function of this quantity is defined by the same expression as the energy distribution function, Eq. (14), in which we substitute $\delta\{\Theta-\partial^2[\delta E(u)]/\partial u\,\partial h\}$ instead of $\delta[E-\delta E(u)]$. We shall not repeat the mathematical details of the derivation, which is analogous to the derivation of Eq. (26) for the conditional distribution function of energy E. The final result for the conditional distribution function of Θ for wells with given stiffness Λ is

$$P(\Theta|\Lambda)=\frac{1}{(2\pi\sigma_\Theta^2)^{1/2}}\exp\left[-\frac{\Theta^2}{2\sigma_\Theta^2}\right], \tag{41}$$

where σ_Θ^2 is defined by

$$\sigma_\Theta^2=g^2L\left\{2\int_0^\infty dr\left[\frac{\partial^2V(r)}{\partial h\partial r}\right]^2-\frac{1}{4m_1(h)}\left[\frac{\partial m_1(h)}{\partial h}\right]^2\right\}. \tag{42}$$

Turning back to Eq. (40), we conclude that the distribution function of the variation of well displacement with the distance between the rods for minima with a given stiffness Λ is Gaussian, with zero average and the second moment

$$\left.\overline{\left(\frac{\partial u}{\partial h}\right)^2}\right|_\Lambda=\frac{\sigma_\Theta^2}{\Lambda^2}. \tag{43}$$

We conclude that whereas soft potential minima undergo arbitrarily large random displacements from their initial positions under small variations of the distance h between the rods, the positions of stiff (and deep) minima change very slightly (as evident from Fig. 2). If one considers the displacement of the most probable minima, one finds that $\overline{(\partial u/\partial h)^2}$ is of order unity, and therefore this displacement is of the same order as the change of the spacing between the rods, δh.

The same procedure can be used to find the change of the well stiffness $\delta\Lambda=(\partial\Lambda/\partial h)\delta h$. Proceeding analogously to the derivation of expression (27), we obtain

$$\left.\overline{\frac{\partial\Lambda}{\partial h}}\right|_\Lambda=\frac{\Lambda}{2}\frac{\partial\ \ln m_2(h)}{\partial h}. \tag{44}$$

In order to obtain the dependence of the stiffness of the average potential well on the distance h between rods, we integrate this equation and obtain

$$\overline{\Lambda}(h)=\overline{\Lambda}(h_0)[m_2(h)/m_2(h_0)]^{1/2}. \tag{45}$$

In the unscreened Coulomb case the stiffness of an average minimum is a strongly decreasing function of the distance between the rods, $\overline{\Lambda}(h)\sim h^{-5/2}$. Equation (45) shows that the distribution $\mathcal{P}(\Lambda)$ of the radii of curvature of the energy minima, Eq. (25), is invariant with respect to the change of the distance between rods. Thus, when the two rods approach each other, existing minima do not disappear and become progressively stiffer and deeper. At the same time, new shallow minima appear, and grow in depth as h is reduced. It is interesting to note that while the former behavior (deepening of existing energy minima) would be observed even if the charges on the two rods were placed on periodic lattices, the appearance of new minima upon closer approach is a characteristic signature of the randomness of the two charge distributions.

D. Scaling estimate

The above observations allow us to introduce a scaling estimate which takes a particularly simple form in the case of unscreened Coulomb interaction between the rods. If we are not interested in the details of the distributions of the parameters of the energy minima but only in the averages of these parameters over the frozen charge distributions, we can replace the microscopic charge distribution by one that is coarse grained over a length scale h (the distance between the rods). Each such electrostatic ''blob'' contains gh charges of both signs, and thus the total charge per blob is of order $Q_h=\pm(gh)^{1/2}$. Since there are L/h such blobs, and the average interaction energy between the rods vanishes (assuming that there is no net charge on the rods), δE can written as the sum of interaction energies of L/h neighboring blobs on the two rods. Each one of the contributions is a random function which takes the values $\pm Q_h^2/h$, and therefore the total interaction energy is also a random quantity with zero average and characteristic deviation

$$\delta E\simeq\pm\left(\frac{L}{h}\right)^{1/2}\frac{Q_h^2}{h}=\pm g\left(\frac{L}{h}\right)^{1/2}, \tag{46}$$

in agreement with the exact result, Eq. (29).

The above scaling picture can be used to answer the following question: let us assume that the system ''sits'' in one of the characteristic minima with energy $\overline{\delta E}_{\min}$ given by Eq. (29). How many charges on the shorter rod must change their positions for this minimum to disappear? This number, τ, can be estimated as follows. The interaction energy can be increased by changing the charge distribution in a way that decreases the attraction or increases the repulsion between each of the two neighboring blobs on different chains. The change of the interaction energy associated with this redistribution of charges $\tau Q_h/h$ should then be equated to $|\overline{\delta E}_{\min}|$. This gives

$$\tau\simeq\sqrt{gL}\ll gL, \tag{47}$$

i.e., the number of charges that should be rearranged for the minimum to disappear is of the order of the square root of the total number of charges on the shorter rod (and does not depend on the distance between the rods). This estimate may be relevant to biological systems in which the effective interaction between the objects can be controlled by biochemical means (e.g., by protonation, phosphorylation, etc. [7]).

IV. PARALLEL PLATES

A. General analysis

In the case of two parallel plates we can transform the sum over the positions of energy extrema in Eq. (11) into an integral over the continuous variable $\mathbf{u}$,

$$\sum_{\text{ext}}\cdots=\int d\mathbf{u}\ \delta\{\partial[\delta E(\mathbf{u})]/\partial\mathbf{u}\}\det[E_{\alpha\beta}(\mathbf{u})]\cdots$$

$$=\int d\mathbf{u}\ \delta\{\partial[\delta E(\mathbf{u})]/\partial\mathbf{u}\}\Lambda_-(\mathbf{u})\Lambda_+(\mathbf{u})\ldots, \tag{48}$$

where the matrix $E_{\alpha\beta}$ is defined in Eq. (8). The minimal Λ_- and the maximal Λ_+ eigenvalues of this matrix were defined in Eqs. (9) and (10). Analogously to the one-dimensional case, Eq. (13), we use the equality

$$\Lambda_-(\mathbf{u})\Lambda_+(\mathbf{u})\theta[\Lambda_-(u)]=\int_0^\infty d\Lambda_-\int_{\Lambda_-}^\infty d\Lambda_+\Lambda_-\Lambda_+ \times\delta[\Lambda_--\Lambda_-(\mathbf{u})] \times\delta[\Lambda_+-\Lambda_+(\mathbf{u})], \tag{49}$$

Substituting Eqs. (49) and (48) into Eq. (11), and changing the order of averaging over $\delta\rho_2$ and integration over $\mathbf{u}$ (which gives the area A' of the infinite plate), we obtain the following representation for the energy distribution function

$$\overline{N_{\min}(E)}=A'\int_0^\infty d\Lambda_-\int_{\Lambda_-}^\infty d\Lambda_+\Lambda_-\Lambda_+ \times\int\int\int dE_+dE_-dE_{xy}\Psi(E,E_+,E_-,E_{xy}) \times\delta(\Lambda_--E_++\sqrt{E_-^2+E_{xy}^2}) \times\delta(\Lambda_+-E_+-\sqrt{E_-^2+E_{xy}^2}). \tag{50}$$

Later we will show that the function

$$\Psi(E,E_+,E_-,E_{xy}) \equiv\frac{1}{\mathcal{N}}\int D[\delta\rho_2]e^{-S[\delta\rho_2]}\delta\left\{\frac{\partial[\delta E(u)]}{\partial\mathbf{u}}\right\} \times\delta[E-\delta E(\mathbf{u})]\prod_j\delta[E_j-E_j(\mathbf{u})] \equiv\Psi(E,\Lambda_-,\Lambda_+) \tag{51}$$

depends on $E_\pm$ and E_{xy} only through their combinations Λ_- and Λ_+, Eqs. (9) and (10), and therefore, it can be moved outside the integrals over $E_\pm$ and E_{xy} in Eq. (50). Performing these integrations, we recast Eq. (50) in the form

$$\overline{N_{\min}(E)}=\frac{\pi A'}{2}\int_0^\infty d\Lambda_-\int_{\Lambda_-}^\infty d\Lambda_+\Lambda_-\Lambda_+ \times(\Lambda_+-\Lambda_-)\Psi(E,\Lambda_-,\Lambda_+). \tag{52}$$

We use the following exponential representation of the δ functions in Eq. (51):

$$\delta[E-\delta E(\mathbf{u})]=\int\frac{dk}{2\pi}\exp\{ik[E-\delta E(\mathbf{u})]\}, \tag{53}$$

$$\delta\left\{\frac{\partial[\delta E(\mathbf{u})]}{\partial u}\right\}=\int\frac{d\mathbf{p}}{(2\pi)^2}\exp\left\{-i\mathbf{p}\cdot\frac{\partial[\delta E(\mathbf{u})]}{\partial\mathbf{u}}\right\},$$

$$\delta[E_j-E_j(\mathbf{u})]=\int\frac{dq_j}{2\pi}\exp\{iq_j[E_j-E_j(\mathbf{u})]\}.$$

Substituting these expressions into Eq. (51), performing the Gaussian integration over the density distribution $\delta\rho_2(\mathbf{x})$, and using the two-dimensional analog of Eq. (18), we obtain

$$\Psi(E,E_+,E_-,E_{xy}) =\int\frac{dk}{2\pi}\int\frac{d\mathbf{p}}{(2\pi)^2}\prod_j\int\frac{dq_j}{2\pi} \times\exp\left\{ikE+i\sum_j q_jE_j-\frac{g^2A}{2} \times[\mathbf{p}^2m_1'(h)+k^2m_0'(h)+(2q_+^2+q_-^2+q_{xy}^2)m_2'(h) -2kq_+m_1'(h)]\right\}, \tag{54}$$

where the integrals $m_k'(h)$ are defined by expressions

$$m_0'(h)\equiv2\pi\int_0^\infty dr\ rV^2(r),\quad m_1'(h)\equiv\pi\int_0^\infty dr\ r\left[\frac{\partial V(r)}{\partial r}\right]^2, \tag{55}$$

$$m_2'(h)\equiv\int_0^\infty dr\ r\left[\frac{\partial^2V(r)}{\partial r^2}-\frac{1}{r}\frac{\partial V(r)}{\partial r}\right]^2.$$

The above moments can be evaluated explicitly in the case of screened Coulomb interaction between the plates. We find

$$m_0'(h)=2\pi\ \mathrm{Ei}(2\kappa h),$$

$$m_1'(h)=\pi\kappa^2\left[e^{-2\kappa h}\frac{(1+2\kappa h)}{(2\kappa h)^2}-\mathrm{Ei}(2\kappa h)\right], \tag{56}$$

$$m_2'(h)=\pi\kappa^4\left[\mathrm{Ei}(2\kappa h)+\frac{e^{-2\kappa h}}{8(\kappa h)^4} \times(3+6\kappa h+2\kappa^2h^2-4\kappa^3h^3)\right],$$

where Ei denotes the exponential integral function.

As can be directly checked from Eq. (54), the function Ψ depends on values E_+ and $E_-^2+E_{xy}^2$ and, therefore, on Λ_- and Λ_+ only. Performing the Gaussian integrations in Eq. (54) and substituting the resulting function $\Psi(E,\Lambda_-,\Lambda_+)$ in Eq. (52), we finally find

$$\overline{N_{\min}(E)}=A'\overline{c}\int_0^\infty d\Lambda_-\int_0^\infty d\Lambda_+\mathcal{P}(\Lambda_-,\Lambda_+)P(E|\Lambda_-+\Lambda_+), \tag{57}$$

The average (surface) concentration of potential wells is given by

$$\overline{c}=\frac{1}{2\pi\sqrt{3}}\frac{m_2'(h)}{m_1'(h)}. \tag{58}$$

For the unscreened Coulomb case this yields $\overline{c}\simeq h^{-2}$, and the number of energy minima is of order A'/h^2. At distances exceeding the screening length we obtain $\overline{c}\simeq\kappa/h$. In Fig. 4 we plot this concentration as a function of the distance between the plates, for several values of the screening length κ^{-1}.

The function $\mathcal{P}(\Lambda_-,\Lambda_+)$ is the normalized probability distribution to find a potential well with two principal inverse

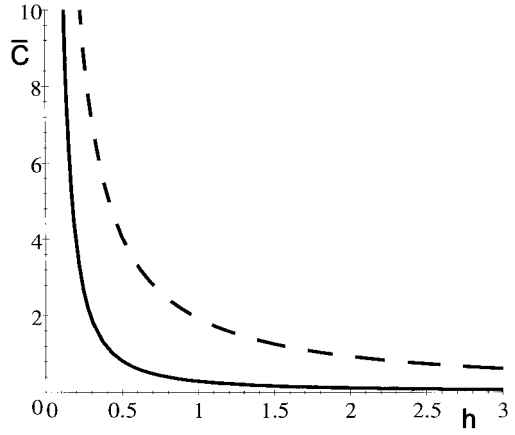

FIG. 4. Plot of the concentration of energy minima $\overline{c}$ as a function of the vertical separation between the plates h (in arbitrary units of length). The solid line corresponds to $\kappa=1$, and the broken line to $\kappa=10$.

squared radii of curvature Λ_- and $\Lambda_+>0$ (here we write out this function in a symmetrized form with respect to Λ_- and Λ_+),

$$\mathcal{P}(\Lambda_-,\Lambda_+)=\left(\frac{3}{\pi}\right)^{1/2}\frac{\Lambda_-\Lambda_+|\Lambda_+-\Lambda_-|}{16[g^2Am_2'(h)]^{5/2}}\times\exp\left[-\frac{3\Lambda_-^2+3\Lambda_+^2-2\Lambda_-\Lambda_+}{16g^2Am_2'(h)}\right]. \quad (59)$$

This function is peaked about $\Lambda_+\simeq 3g[Am_2'(h)]^{1/2}$ and $\Lambda_-\simeq 1.34g[Am_2'(h)]^{1/2}$ (i.e., the most probable energy wells are asymmetric) and vanishes for large and small $\Lambda_\pm$. In Eq. (22), $P(E|\Lambda_-+\Lambda_+)$ is the conditional probability to find the energy minimum with energy E if its inverse squared principal radii of curvature are Λ_- and Λ_+ [it depends only on the mean stiffness, $(\Lambda_-+\Lambda_+)/2$]:

$$P(E|\Lambda_-+\Lambda_+)=\frac{1}{(2\pi\sigma_E^2)^{1/2}}\exp\left[\frac{-[E-\overline{\delta E}(\Lambda_-+\Lambda_+)]^2}{2\sigma_E^2}\right], \quad (60)$$

where the average energy of a well with the given Λ_- and Λ_+ is

$$\overline{\delta E}(\Lambda_-+\Lambda_+)=-\frac{m_1'(h)}{m_2'(h)}\frac{\Lambda_-+\Lambda_+}{2}<0, \quad (61)$$

and the standard squared deviation of energy from this average

$$\sigma_E^2=g^2A[m_0'(h)-m_1'^2(h)/(2m_2'(h))]. \quad (62)$$

For unscreened Coulomb interaction between the plates, $\sigma_E^2\simeq g^2A\ln(A'/h^2)$. This logarithmic divergence disappears in the case of a finite screening length κ^{-1}. In the limit $h\ll\kappa^{-1}\ll(A')^{1/2}$, the above logarithm is replaced by $2\ln(1/\kappa h)$. For rod separations exceeding the screening length, σ_E decreases exponentially with κh.

Averaging Eq. (61) over $\Lambda_\pm$ with the distribution function (59), we obtain the average well depth

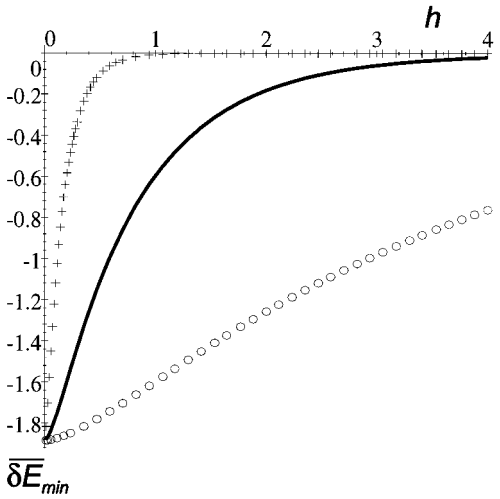

FIG. 5. Plot of the average energy of the minima, $\overline{\delta E}_{\min}$ (in units of $gA^{1/2}$), as a function of the separation between the plates h (in arbitrary units of length, for different values of the inverse screening length κ: 1 (solid line), 0.2 (circles), and 5 (crosses).

$$\overline{\delta E}_{\min}=-8gm_1'(h)\left(\frac{A}{3\pi m_2'(h)}\right)^{1/2}. \quad (63)$$

As in the two-rod case, the average height of energy maxima is simply $\overline{\delta E}_{\max}=-\overline{\delta E}_{\min}$. Symmetry considerations imply that the average value of the energy corresponding to saddle points is zero.

In the unscreened Coulomb case, Eq. (63) gives $\overline{\delta E}_{\min}\simeq gA^{1/2}$, independent of the distance between the plates. As expected, the average depth of the energy minima decays exponentially with the separation between the plates at distances exceeding the screening length (Fig. 5). Finally, we would like to stress that, contrary to the usual consideration of electrostatic interactions between two charged plates, where the presence of electrical double layers must be taken into account [8], such effects are unimportant for randomly charged plates, where the total charge in any finite region of the plates vanishes on the average, and condensation of free counterions on the plates is not expected to play an important role.

B. Stick slip

Up to this point we considered the case of two randomly and irreversibly charged objects, and assumed for simplicity that the total charge on each object vanishes. A different situation which may, in principle, be realized in experiments utilizing the surface force apparatus (when the device operates in the shear mode [9]), is when the two parallel interacting surfaces are randomly charged, with average charge density $\overline{\rho}$. In this case there will be average electrostatic repulsion between the plates, and one has to apply a normal force in order to maintain the separation between them.

What happens if we attach a spring to one of the plates (say plate 2, with area A') and move the other plate (plate 1, with area A) by a distance u parallel to it? If the distribution of charge on the plates is uniform, there will be no restoring forces associated with this displacement, and plate 2 will not move. We now assume that the charge distributions on the

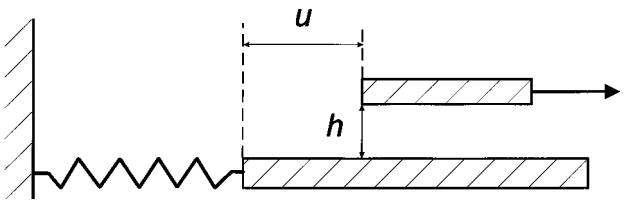

FIG. 6. Schematic drawing of a stick-slip type experiment. The two plates are separated by a distance h, and undergo parallel translation by a distance u.

two plates are randomly frozen (and uncorrelated) and proceed to analyze the response of plate 2 to the displacement of plate 1 (see Fig. 6).

As we have showed in Sec. IV A, the presence of frozen random charge distributions on the plates leads to the appearance of a large number of energy minima which correspond to different relative parallel displacements of the plates. Since, for macroscopic plates, the typical energy associated with these minima scales as $A^{1/2}$, for sufficiently large plates it can be much larger that the thermal energy k_BT and the plates will ''get stuck'' in one of the minimal energy configurations. The electrostatic repulsion between the plates scales as A and, therefore, the normal force needed to keep the plates at a fixed separation from each other will be dominated by the average repulsion, and will not be significantly affected by the relative displacement.

The presence of these minima will lead to the appearance of macroscopic restoring forces for relative displacement of the plates [10]. We showed earlier that the depth of an energy minimum has a typical value $\overline{\delta E}_{\min}$ [Eq. (63)]. Since such energy wells are densely distributed with respect to the relative displacement of the plates, the system will occupy one of these characteristic minima. Plate 2 will move together with plate 1 (stick phase) until the force on it exceeds some critical value $f_{\rm crit}$ at which point it will recoil back (slip). This value can be estimated from the characteristics of the typical energy well:

$$f_{\rm crit} \simeq \left[\overline{\left(\frac{\partial E(u)}{\partial u} \right)^2} \right]^{1/2} = g \sqrt{A m_1'(h)},$$

where $m_1'(h)$ is defined in Eq. (56). For unscreened Coulomb interactions this yields the simple relation $f_{\rm crit} \simeq g A^{1/2}/h$. In the presence of screening this force decays exponentially with separation between the plates, and stick slip is expected only at separations $h \leqslant \kappa^{-1}$ (and can be suppressed by the addition of salt).

When the critical force is exceeded, plate 2 will recoil back to a position in which the spring force becomes sufficiently small. The process will repeat itself as long as we continue to drag plate 1, and stick-slip motion of plate 2 will be observed. Note that each time the critical spring force is exceeded, plate 2 recoils to a new position which corresponds to one of the typical energy minima and, since, in general, there are many such minima, a statistical spread of equilibrium positions of the lower plate will result.

Note that the value of the critical force depends only on the properties of the energy landscape of the interacting plates, and not on experimental details such as the spring constant, etc. Our estimate of the critical force defines the minimal force that has to be applied in order to initiate relative motion of the two plates. This force is analogous to static friction between two solids in contact.

V. CORRELATED DENSITY PATTERNS AND RECOGNITION AT A DISTANCE

Up to this point we assumed that the random distributions of frozen charges on the plates are uncorrelated. We now consider a different class of problems, i.e., the case of strong correlation between the charge distributions on the plates. In particular, we will consider a situation which has an important analog in biology, namely, that of two plates which would stick to each other when brought into contact in a particular relative orientation (the random version of the ''lock and key'' principle).

Consider two identical circular discs of area A such that the charge distribution on one disc is the mirror image of that on the other one (the charge distributions are identical except that each positive charge on one disc is replaced by a negative one on the other, and vice versa). This charge distribution is random and frozen and we assume that the total charge on each of the discs vanishes. This system has a well-defined minimal energy configuration at contact, namely, that of exact overlap of the two mirrored charge distributions. We now proceed to calculate the energy landscape for two such parallel discs of radius R separated by a horizontal distance u and a vertical distance h and rotated by an angle φ with respect to the direction which corresponds to exact overlap of the two charge distributions.

Under the conditions of the model, the number density of charges on disc 1, $\rho_1(x,y)$, is a random quantity with quenched average

$$\overline{\rho_1(x,y)\rho_1(x',y')} = g\,\delta(x-x')\,\delta(y-y'), \tag{64}$$

and ρ_2 is related to it by translation and rotation,

$$\rho_2(x,y) = \rho_1(u_x + x\,\cos\varphi + y\,\sin\varphi, u_y - x\,\sin\varphi + y\,\cos\varphi), \tag{65}$$

where u_x and u_y are the components of the relative displacement of the two disks in the plane parallel to the discs. Since the charge distributions on the two plates are correlated, the quenched average of the energy $E(\varphi,h,u)$ [defined in Eq. (1)] does not vanish. For the unscreened Coulomb case it is given by

$$\overline{E}(\varphi,h,u) = -g \int_0^{2\pi} d\theta \int_0^R \frac{r\,dr}{\sqrt{u^2 + h^2 + 4r^2\,\sin^2(\varphi/2) + 4ru\,\sin(\varphi/2)\sin\theta}}. \tag{66}$$

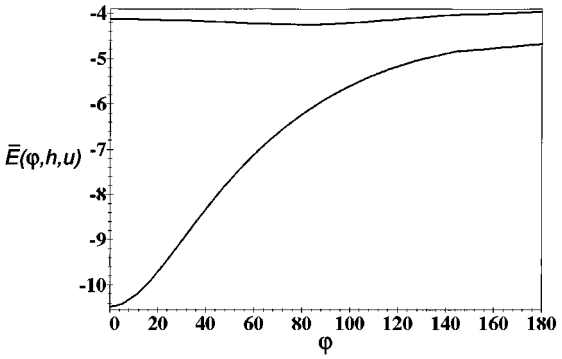

FIG. 7. Plot of the average interaction energy $\overline{E}(\varphi,h,u)$ as a function of the angle φ (in deg) which describes the deviation of the mirror imaged charge distributions on the two discs from perfect alignment. The distance between the discs is $h=0.6R$, and their relative displacement is $u=0$ (lower curve) and $1.4R$ (upper curve).

In Fig. 7 we plot the dependence of the interaction energy $E(\varphi,h,u)$ as a function of the angle φ, for $h=0.6R$ and $u=0$ and $1.4R$. Note that the minimum at $\varphi=0$ $(u=0)$, which corresponds to perfect alignment of the charge distributions, is much deeper than that at finite φ $(u=1.4R)$. The angular width of this minimum (at $\varphi=0$) decreases with separation, and becomes vanishingly small in the limit $h/R\rightarrow 0$. Thus, although the depth of the minimum increases when the two disks approach each other, a random search of the ''correct'' (i.e., minimal energy) configuration becomes increasingly hard.

Although the above integrals cannot be calculated analytically, several comments can be made about the angular dependence of the minima for different separations between the discs. For relative displacements $u<\sqrt{2}h$, the energy reaches its absolute minimum over φ at $\varphi=0$, which corresponds to perfect orientation of the two disks (the two distributions can be brought into coincidence by pure translation, without rotation). When the ratio $u/\sqrt{2}h$ becomes larger than unity, the minimum is attained at a finite angle $\pm\varphi^*$, which increases with this ratio. An analytical expression for this angle can be obtained when $u/\sqrt{2}h$ is only slightly larger than unity. In this regime,

$$\varphi^*=2\left(\frac{9}{7}\right)^{1/2}\frac{h}{R}\left(\frac{u}{\sqrt{2}h}-1\right)^{1/2}. \tag{67}$$

Note that this angle is proportional to h/R, and tends to zero when the vertical distance between the discs becomes much smaller than its radius (strong overlap regime).

Another analytical result can be obtained in the limit $u\gg h$ and $h\ll R$. In this case we obtain

$$\varphi^*=\begin{cases} 2\arcsin(u/R) & \text{when} \quad u\leqslant R \\ \pi & \text{when} \quad u>R, \end{cases} \tag{68}$$

i.e., the angle φ^* varies continuously from zero to π when the centers of the two nearly overlapping discs separate by a horizontal distance corresponding to their radius.

Numerical investigation shows that a similar phenomenon takes place when u increases at any fixed vertical separation h: when u exceeds $\sqrt{2}h$, the angle φ^* becomes finite, and increases to π at some value of u determined by the relative

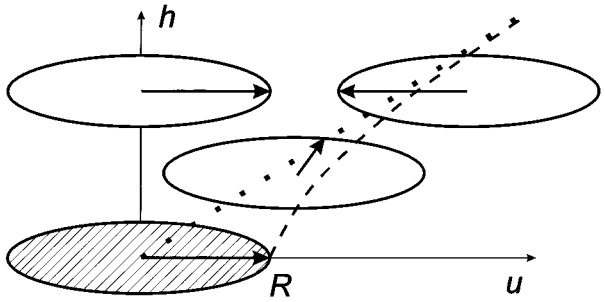

FIG. 8. Schematic picture of the relative orientation of the mirror imaged charge distributions on the two discs. One of the discs (shaded) is fixed at the origin, and the relative orientation of the other disc, corresponding to the minimal energy configuration for different displacements, is shown. The orientations of the minima are $\varphi^*=0$ in the region to the left of the dotted curve and $\varphi^*=\pi$ to the right of the dashed curve. The region between the two curves corresponds to $0<\varphi^*<\pi$.

elevation h. For large vertical separations, $h\gg R$, the change from $\varphi^*=0$ to $\varphi^*=\pi$ takes place in a narrow interval close to the line $u=\sqrt{2}h$. Thus, when two plates approach each other from infinity at a fixed vertical distance h, the relative angle φ^* corresponding to the energy minimum rotates from π to zero (see the schematic drawing, Fig. 8) and the minimum becomes progressively deeper. The physical reason for this angular dependence of the energy becomes clear if we replace the charge distribution on each plate by a dipole, and consider the interaction between two such dipoles. According to our mirror image construction, when the two discs are placed above each other, the minimal energy configuration corresponds to $\varphi=0$, i.e., the orientations of the two dipoles are opposite to each other (in Fig. 8, the arrow on the lower disc gives the direction of its dipole moment; the arrow on the upper disc points opposite to its dipole moment). When they are displaced horizontally far enough from each other, the minimal energy configuration becomes one in which the dipoles point along the same direction $(\varphi=\pi)$. The range at which the minimum occurs at a finite value of φ corresponds to relative positions of the discs in which the multipolar contributions to the interactions between the two frozen charge distributions dominate over the dipolar ones. This range becomes narrower with increasing vertical separation and, at sufficiently large separations, a nearly discontinuous transition from $\varphi=\pi$ to $\varphi=0$ is expected to take place when $u\rightarrow\sqrt{2}h$.

Up to this point we considered only the quenched average of the interaction energy between the discs (''coherent'' contribution). In principle, we should also consider the mean square deviation from this average, $\overline{\delta E^2}$ (''incoherent'' contribution). It can be shown that such incoherent contributions are of the same order as the coherent ones for disc separations much larger than their diameter. However, the interaction between the discs becomes strong only when the separation between them is significantly smaller than their dimension (R). In this range the ratio of the coherent to the incoherent contributions is of order $R/\sqrt{h^2+u^2}$, and the incoherent contribution is negligible. At such separations the minimal energy configuration always corresponds to nearly perfect alignment of the charge distributions on the two discs, $\varphi=0$.

In the above analysis we assumed perfect correlation between the frozen charge distributions on the two plates. If the charges on the two discs are only partially correlated, the attractive interaction will be reduced by a factor α proportional to the fraction of the correlated charges, and the incoherent contribution to the energy will remain unchanged. The ratio of coherent to incoherent contributions will be reduced by a factor α, and therefore a strong energy minimum corresponding to alignment of the coherent charge distributions will now appear only when the discs approach separations of order αR. Thus perfect recognition of the correlated parts of the charge distributions on the two discs will still take place when they are brought into contact.

The discussion in this section may appear to be based on a somewhat artificial model, since the preparation of such mirror imaged randomly frozen charge distribution may pose formidable difficulties. Note, however, that since the theory makes no assumptions about the dimensions of the charged objects, one can construct such a system by assembling a random array of negative and positive electrodes and then constructing its mirror image. Another example to which the general methodology described in this section can be applied is that of an array of parallel magnets with their north and south poles randomly alternating along the normal to the array. A ''mirror image'' of this random array can be prepared in a thin ferromagnetic film which consists of disordered magnetic domains (with directions pointing randomly in and out of the surface of the film), if this film is brought near the Curie temperature and placed in contact with the random magnetic array. A mirror image of the array will form in the film, and can subsequently be frozen by decreasing the temperature. The resulting magnetic interactions between the film and the array will vary with their separation and relative orientation in a manner closely resembling our electrostatic model.

Finally, one can try to speculate on the relevance of our model to recognition in biological systems. Although many different types of attractive and repulsive interactions (electrostatic, hydrophobic, hydrogen bonding, van der Waals, etc.) are present in these systems [11], the resulting potential energy surfaces can be modeled by introducing random (or partially correlated) distributions of effective charges. The justification for this statement is that the random combination of attractive and repulsive long range forces in our theory can give rise to effective interaction potentials of arbitrary complexity and, therefore, the theory can serve as a generic model of interactions between biological systems in which perfect ''lock-and-key'' arrangement of the two objects at contact is preceded by prealignment at a distance, when the separation of the approaching objects becomes of the order of their dimensions (or on the order of the Debye screening length, in the presence of salt). This prealignment can provide a mechanism by which metastable ''traps'' at contact can be avoided by sensing the energy landscape at distances where the energy barriers are small enough to allow the system to find the true energy minimum (for example, when the depth of the coherent minimum is larger than k_BT and the depths of the incoherent ones are smaller than k_BT, at separations of the order of the size of the objects).

VI. DISCUSSION

We studied the energy landscape generated by relative translation of two random frozen charge distributions interacting through long range electrostatic forces. Two simple geometries were considered, for which the statistical properties of this energy landscape can be calculated analytically, namely, two parallel rigid rods and two parallel rigid plates. We first examined the case of completely uncorrelated charge distributions on the two objects. We found that when the total charge on each of the objects vanishes and the Coulomb interaction between them is unscreened (i.e., when there is no characteristic length scale associated with the interaction potential), the interaction between the objects becomes significant and energy minima appear when the separation between these objects becomes of the order of their dimensions (when the two objects are of different sizes, this happens when the separation is of the order of the linear dimensions of the larger of the two). When the separation is further decreased, these energy wells deepen, and new wells appear. We calculated the distributions of energy minima, the depth and the width of the characteristic energy wells, and the spacing between them, and showed that both the width and the spacings are of the order of the separation between the objects. This indicates that the typical energy wells are densely packed in the space generated by the relative translation of the objects.

The above considerations apply to separations down to the average distance between the charges ($h \geqslant g^{-1}$ for rods and $h \geqslant g^{-1/2}$ for plates, respectively), at which point our assumption of continuous charge distributions on the objects breaks down. Strictly speaking, there is also an upper cutoff on the distance between the objects; as shown in the Appendix for the two-rod case, the method of averaging over frozen disorder used in this work becomes inaccurate for separations which exceed the linear dimension of the longer rod, $h \geqslant L'$. Although, at larger separations, intermittency effects not considered in this work may become important, such corrections are of limited physical interest since in this limit the average number of energy minima is of order unity and their depth tends to zero. A more restrictive condition follows from the fact that we did not explicitly introduce the constraint of fixed total charge on each of the rods (we assumed that it is fixed and, consequently, did not average over the distribution of total charge on the rods). It can be shown that accounting for the fixed total charge constraint leads to corrections of order h/L (L is the length of the shorter rod) to our results. These corrections produce a constant shift of the energy, and do not depend on the relative displacement of the objects, u.

We found that although much deeper energy minima than the typical ones may also exist, the probability of encountering them is exponentially small and they may or may not be observed in finite size systems, depending on the strategy by which the energy landscape is investigated. If two objects approach each other in an adiabatic and unconstrained fashion, due to temperature fluctuations or other sources of random noise, they will be captured by the lowest minimum (it is the first minimum to appear when the separation between them is of the order of their size), whose depth increases and whose position becomes pinned down (at some relative dis-

placement **u**) upon further approach. When the experiment is repeated, the relative position of the two objects at contact will be faithfully reproduced. A different scenario takes place if the relative displacement of the randomly charged objects is varied with some finite precision by externally applied forces (allowing for small fluctuations of this displacement). In this case, the system will jump between the most probable energy minima and will not be able to find the lowest one. Since the number of these minima at contact is proportional to the number of charges on the objects, the relative positions at contact will not be reproduced when the experiment is repeated. The conclusion, that a random search of the ground state of interacting random objects is more efficient than any deterministically driven one, may have interesting implications for biology and for information theory. A serious consideration of these questions is beyond the scope of this work, and requires a thorough study of the corresponding kinetics.

In the preceding paragraph we discussed the application of our model to studies of ''recognition'' for two uncorrelated objects, in which one looks for an *a priori* unknown spatial arrangement that optimizes the overlap between the two frozen charge distributions. We also studied a different limit of this problem, namely, that of perfectly correlated charge distributions (mirror images), for which the optimal overlap configuration at contact is known and one would like understand how this configuration is attained when the two objects approach each other. We found that the presence of long range forces leads to remote ''sensing'' of correlations, and raises the possibility of prealignment into the ground state configuration before contact. The characteristic separation at which the objects begin to sense the optimal relative orientation is comparable to their linear dimension. If the correlation between the charge distributions becomes imperfect due to the presence of defects, the sensing distance is reduced and, since the depth of the incoherent minima increases with decreasing separation between the objects, the system may fall into one of these ''false'' minima, and alignment between the correlated portions of the objects will be prevented. When the concentration of defects is further increased, the ground state configuration will no longer be determined by the correlated charges, but rather by one of the incoherent minima, and random alignment at contact will result (the case discussed in the previous paragraph).

Finally, we considered a situation of the type encountered in studies of the physics of friction, and evaluated the typical minimal force needed to produce parallel displacement of two randomly charged plates separated by a distance h from each other. When the separation between the plates is sufficiently small, the system will be trapped in a configuration that corresponds to one of the multiple energy minima, and relative motion will occur only when the magnitude of the force exceeds some critical value that depends on the height of the energy barriers. As a result, stick-slip motion will occur under typical experimental conditions. This phenomenon is the analog of static friction between solids in contact. A complete treatment of solid friction, including dynamic friction, must account for the energy dissipation produced by this relative motion, and is beyond the scope of this work.

Our theory applies to objects of arbitrary size (microscopic as well as macroscopic). Although in this work we analyzed in detail the case of screened Coulomb interactions between the rods (and between the plates), the generalization to other types of interaction potentials is straightforward (we only need to know the second moments of the potential and of its derivatives). The combination of long range attractive and repulsive forces can be used to generate interaction energy landscapes of nearly arbitrary shape, and can serve as a generic model for describing more complicated situations in which many types of interactions (e.g., electrostatic, hydrophobic, van der Waals, etc.) act simultaneously. The main ideas of this work can be applied to situations frequently encountered in biological systems, where the distribution of the effective ''charges'' is fixed by chemistry, such as interactions between the surfaces of bacteria, interactions between folded proteins (in the latter case, temperature effects which were not considered here, have to be taken into account), and other. One may object that our assumption of continuous charge distributions does not apply to ''small'' systems such as proteins which contain, at most, several hundreds of amino acids. However, from the perspective of quantum chemistry, each amino acid is a ''large'' molecule which is characterized by a complicated potential energy surface. Furthermore, the potential field in the vicinity of an amino acid depends on the details of the local environment in which this molecule is located, e.g., on its neighbors within the primary, secondary, and tertiary structure of the protein, on the PH, etc. When viewed at this resolution, the potential field which exists in the vicinity of a large protein may be not too different from that generated by a randomly frozen charge distribution of the type considered in this work. We cannot, of course, be certain at present that nature utilizes such long range interactions (their range is determined by the screening length) for recognition by prealignment, yet the possibility that this is the case gives some hope that future extensions of the present model may have important implications for biology.

ACKNOWLEDGMENTS

This work was motivated by discussions with Manfred Wilhelm, who suggested that stick-slip motion may arise due to the presence of frozen charge distributions on the plates (cleaved mica plates have potassium ions on their surface, which dissociate in aqueous environment leaving behind negatively charged surfaces). We would like to thank Isaac Freund, Ido Kanter, Yacov Kantor, and Aleksei Tkachenko for helpful comments and discussions. S.P. would like to thank the Department of Physics, Bar-Ilan University, for hospitality during his stay in Israel where this work was done. Y.R. acknowledges financial support through a grant from the Israel Science Foundation.

APPENDIX

In Sec. II we replaced $N_{\min}(E)$ with its average over the ensemble of objects with quenched disorder. In general, the above procedure is questionable because of the possibility of *intermittency* which occurs when the main contribution to averages comes from atypical configurations of the disordered system and, therefore, the value of some physical quantities in a typical realization of the disorder cannot be

represented by its average over the quenched ensemble (see, for example, spin glasses [2]). We proceed to check whether such problems arise in our model.

Consider the variation of the number of energy minima per unit energy, $N_{\min}(E)$, for different realizations of the disordered charge distribution on the rods. A possible way to check whether intermittent behavior arises in our theory is to estimate higher order moments of the function $N_{\min}(E)$. Repeating the steps which led to Eq. (19), we obtain

$$\overline{N^n_{\min}(E)}=\prod_{q=1}^{n}\left[\int_0^{L'}du_q\int_0^{\infty}d\Lambda_q\Lambda_q\prod_{j=1}^{3}\int\frac{dk_{qj}}{2\pi}\right]\times\exp\left[i\sum_q k_{q1}E+i\sum_q k_{q3}\Lambda_q-\frac{g^2L}{2}\sum_{jl,qq'}D^{qq'}_{jl}k_{qj}k_{q'l}\right], \tag{A1}$$

$$\mathbf{D}^{qq'}=\mathbf{D}\delta_{qq'}+\mathbf{D}'(1-\delta_{qq'}). \tag{A2}$$

Here the matrix $\mathbf{D}$ is defined in Eq. (20), and $\mathbf{D}'$ depends on $u_q-u_{q'}$,

$$\mathbf{D}'=\begin{pmatrix} m_0(h)\,\eta_0(u_q-u_{q'}) & 0 & -m_1(h)\,\eta_1(u_q-u_{q'}) \\ 0 & m_1(h)\,\eta_1(u_q-u_{q'}) & 0 \\ -m_1(h)\,\eta_1(u_q-u_{q'}) & 0 & m_2(h)\,\eta_2(u_q-u_{q'}) \end{pmatrix}. \tag{A3}$$

The function $\eta_0(u)$ is given by expression

$$\eta_0(u)\equiv\frac{1}{m_0}\int_{-\infty}^{\infty}dr\ V(r)V(r+u), \tag{A4}$$

and the integrals η_1 and η_2 are defined in Eq. (33).

Note that if we neglect the nondiagonal term $\mathbf{D}'$ in Eqs. (A1) and (A2), we obtain $\overline{N^n_{\min}(E)}\simeq[\overline{N_{\min}(E)}]^n$. We can estimate the contribution of this term by treating it as a small perturbation. To first order in $\mathbf{D}'$, we obtain

$$\overline{N^n_{\min}(E)}=[\overline{N_{\min}(E)}]^n\left\{1+\frac{g^2L}{L'}\,\frac{n(n-1)}{2}\times\left[\frac{\partial\,\ln\overline{N_{\min}(E)}}{\partial E}\int_{-\infty}^{\infty}dr\ V(r)\right]^2\right\}. \tag{A5}$$

This expression can be used to estimate $\overline{\ln N_{\min}(E)}$, which contains information about all the moments, and is, therefore, sensitive to intermittency effects. Using the replica trick, $\ln Z=\lim_{n\to 0}(Z^n-1)/n$ (for arbitrary Z), we obtain

$$\overline{\ln N_{\min}(E)}=\ln\overline{N_{\min}(E)}\times\left\{1-\frac{g^2L}{2L'}\left[\frac{\partial\,\ln\overline{N_{\min}(E)}}{\partial E}\int_{-\infty}^{\infty}dr\ V(r)\right]^2\right\}. \tag{A6}$$

In all physically relevant situations, some degree of screening is present, and the integral over the potential converges. Since $\partial\,\ln\overline{N_{\min}(E)}/\partial E\simeq\sqrt{h/g^2L}$ [see Eq. (30)], the variance of $\ln N_{\min}(E)$ is of order h/L', and we conclude that intermittency effects come into play only when the separation between the rods exceeds the length of the longer rod, i.e., when the average number of energy minima becomes of the order of or smaller than unity. It can be shown that the corresponding correction in the case of two randomly charged plates in the presence of screening is of order $(\kappa^2A)^{-1}$.

[1] V. S. Pande, A. Y. Grosberg, and T. Tanaka, Proc. Natl. Acad. Sci. USA **91**, 12 972 (1994).

[2] M. Mezard, G. Parisi, and M. Virasoro, *Spin Glass Theory and Beyond* (World Scientific, Singapore, 1987).

[3] S. Panyukov and Y. Rabin, Phys. Rep. **269**, 1 (1996).

[4] C. D. Sfatos, E. I. Shakhnovich, and A. M. Gutin, Phys. Rev. E **51**, 4727 (1995).

[5] Y. Kantor and M. Kardar, Phys. Rev. Lett. **14**, 421 (1991).

[6] *Selected Papers on Noise and Stochastic Processes*, edited by N. Wax (Dover, New York, 1954), p. 212, Eq. (36–9).

[7] L. Stryer, *Biochemistry*, 4th ed. (Freeman, New York, 1995).

[8] J. Israelachvili, *Intermolecular and Surface Forces*, 2nd ed. (Academic, London, 1992).

[9] J. Klein, D. Perhia, and S. Warburg, Nature (London) **352**, 143 (1991).

[10] We would like to thank Manfred Wilhelm for bringing this possibility to our attention.

[11] B. Alberts, D. Bray, J. Lewis, M. Raff, K. Roberts, and J. D. Watson, *Molecular Biology of the Cell*, 3rd ed. (Garland, New York, 1994).